

stored in 0.32-cm nylon pressure tubing. Because of capillary mixing, the usable volume is only about 16 ml.

4. All gas analyses were performed on a Hewlett-Packard dual-column gas chromatograph equipped with a sample stripping system and a Carle thermistor detector. The 4-ml sample is stripped with the carrier gas, which is then dried over Drierite; then O₂ + Ar are separated from the other gases on a 1.8-m molecular sieve 5A column at 40°C. The Ar and O₂ are not separated from each other, and thus a small correction for Ar must be made, based on the solubility of Ar in seawater.
5. At two stations, two gas-sampling valves were placed in series at every other depth to obtain an estimate of our overall precision. The mean difference between duplicate measurements was 7 μmole kg⁻¹. Accuracy was estimated by intercalibration against water column samples analyzed by Winkler titration. In addition, our bottom water measurements from the in situ sampler agree to within 2 percent with the Geochemical Ocean Sections Study (GEOSECS) bottom-water O₂ values for this part of the deep Pacific.
6. R. A. Berner, in *The Sea*, E. D. Goldberg, Ed. (Wiley, New York, 1974), vol. 5, pp. 427-450; *Early Diagenesis: A Theoretical Approach* (Princeton Univ. Press, Princeton, N.J., 1980).
7. T. L. Ku, W. S. Broecker, N. Opdyke, *Earth Planet. Sci. Lett.* 4, 1 (1968).
8. N. L. Guinasso and D. R. Schink, *J. Geophys. Res.* 80, 3022 (1975).

9. V. Grundmanis and J. W. Murray, *Geochim. Cosmochim. Acta*, in press.
10. R. E. McDuff and J. M. Gieskes, *Earth Planet. Sci. Lett.* 33, 1 (1976).
11. A. Lerman, *Geochemical Processes: Water and Sediment Environments* (Wiley-Interscience, New York, 1979), p. 96.
12. Calculated from water content and sediment density measurements made by C. Olson and F. L. Sayles (Woods Hole Oceanographic Institution).
13. Estimated from resistivity measurements determined on sediment cores immediately after collection by C. Olson and F. L. Sayles.
14. T. R. S. Wilson, *Nature (London)* 274, 354 (1978).
15. K. L. Smith, Jr., *Mar. Biol.* 47, 337 (1978).
16. K. R. Hinga, J. M. Sieburth, G. R. Heath, *J. Mar. Res.* 37, 557 (1979).
17. J. C. G. Walker, *Am. J. Sci.* 274, 193 (1974).
18. We thank J. Sawlan for assistance in sample collection and M. Bolan for execution. Drs. S. Emerson, R. A. Berner, and F. L. Sayles offered many valuable, critical comments. We thank B. Fulton for typing the manuscript. University of Washington contribution number 1165. This research was supported by grant OCE-78 18746 from the National Science Foundation.
- * Present address: Hawaii Loa College, Kaneohe, Oahu 96744.

19 March 1980; revised 15 May 1980

Surface Charge Heterogeneity in Amphibole Cleavage Fragments and Asbestos Fibers

Abstract. *Aspect ratio and electrophoretic mobility data for amphibole particles reveal that short fibers and blocky cleavage fragments have a smaller net charge than highly elongated particles. Asbestos fibers and cleavage fragments of the same dimensions exhibit the same net negative surface charge but positively charged ends and negatively charged lateral surfaces.*

Research is being done at the Bureau of Mines Twin Cities Research Center on the relation between electrophoretic mobility and the aspect ratio of amphibole fibers and cleavage fragments (1) in an effort to minimize the undesirable occupational hazards associated with mining and mineral processing operations. [The nomenclature used in this report conforms to that suggested by Campbell *et al.* (2).]

In order to determine the relation between surface charge and aspect ratio for a wide range of amphibole particle shapes, experiments were designed to determine both the surface charge and the aspect ratio for individual particles. In the work described here, a microelectrophoresis cell with a rectangular cross section was used so that particles in the field of view could be photographed. Electrophoretic mobility data were obtained for particles with aspect ratios from 1 up to 40. These data gave important insight into the surface charge properties of amphibole particles.

The asbestiform minerals studied were crocidolite and grunerite asbestos from the International Union Against Cancer (IACC) (3). A sample of acicular tremolite (originally from Canaan, Con-

necticut) was obtained from the Science Museum of Minnesota, St. Paul. The Bureau of Mines Research Center at Avondale, Maryland, supplied a sample of riebeckite from El Paso County, Colorado. The IACC samples were used as received, and the acicular tremolite and riebeckite were hand-ground in an agate mortar and pestle. Suspensions in distilled water [0.1 percent (weight-volume)] were prepared by magnetic stirring and ultrasonic agitation. The pH was adjusted to 7 with 0.01M HNO₃ and NaOH, and the mixtures were sealed and allowed to stand for 15 to 20 hours. If needed, the pH was readjusted to 7 just prior to the microelectrophoresis measurements.

Table 1. Limiting values of electrophoretic mobility resulting from the different lateral charge density and basal charge density.

Mineral	μ ₂	μ ₁
	(μm/sec)/(V/cm)	
Grunerite asbestos	-2.8	+5
Crocidolite	-2.8	+4
Fibrous tremolite	-2.5	+2
Riebeckite	-2.5	+1
All points	-2.7	+4

We determined the aspect ratio and surface charge simultaneously, using a rectangular cell electrophoresis system and petrographic microscope equipped with a camera. The rectangular cavity in the cell had a width of 12 mm and a depth of 0.95 mm. The polished platinum electrodes were separated by 7.4 cm, and the microscope had an overall magnification of ×375. The cell was filled with the suspension of amphibole particles and positioned so that the microscope was focused exactly 0.20 mm above the bottom of the cell.

Times were recorded only for elongated particles (aspect ratio of about 3 or greater) that remained parallel with the electric field as they moved. Blocky particles were randomly oriented owing to Brownian movement. The distance traveled was 220 μm, and the voltage was 175 V. The ionic strength was about 10⁻⁴ during these measurements. The shape, location, and orientation of each particle tracked was also recorded so that later it would be possible to determine which specific particle was followed in the resulting photograph. We determined the aspect ratio of each particle by measuring its image in the photograph; one photograph was required for each particle. Particles were usually 0.5 to 2 μm wide and 3 to 15 μm long.

A control experiment was performed to ensure that observed differences in mobility between elongated and blocky particles truly reflected a difference in net surface charge rather than simply a hydrodynamic effect. Grunerite asbestos and crocidolite were suspended in 10⁻³M KNO₃. In both suspensions, the electrophoretic mobilities of blocky particles, elongated particles oriented perpendicular to the electric field, and elongated particles parallel with the field were measured.

For both grunerite asbestos and crocidolite, the elongated particles perpendicular to the electric field had relative electrophoretic mobilities of 0.74 ± 0.03 and 0.7 ± 0.02, respectively, compared with elongated particles parallel to the field. Theory predicts that the electrophoretic mobilities of spherical particles would exactly equal the mean of values of cylinders oriented parallel and perpendicular to the applied field (4). The blocky particles would approximate the behavior of spheres. Thus, on the basis of shape effects only, the mobility of blocky particles of grunerite asbestos and crocidolite were expected to be 0.85 ± 0.03 and 0.87 ± 0.04, respectively, relative to that of elongated particles moving parallel to the field. However, the observed

relative mobilities for blocky particles were 0.57 ± 0.01 and 0.63 ± 0.04 . Since the measured mobility for blocky particles is only about two-thirds the value calculated on the basis of shape factors, the lower measured mobility for blocky particles reflects a smaller net negative charge. Although shape may have been a minor factor in producing the smaller mobilities measured for the particles with the lowest aspect ratios, true surface charge differences were the predominant cause for the observed trend.

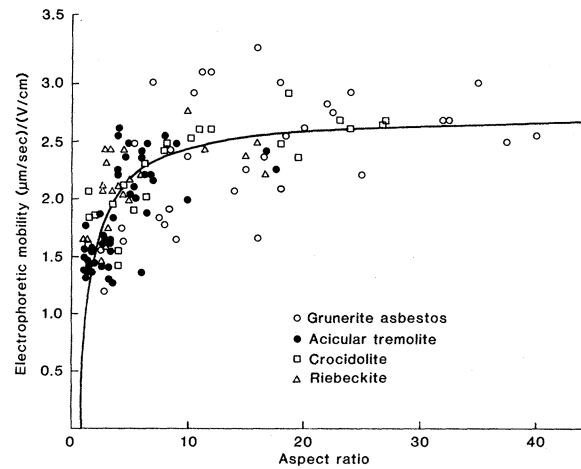
Electrophoretic mobility-aspect ratio data for riebeckite, acicular tremolite, crocidolite, and grunerite asbestos are given in Fig. 1. Each point represents the measured electrophoretic mobility and aspect ratio for one particle. The mobility was lower for blocky particles, but it rapidly increased for particles of higher aspect ratio. All four samples behaved in the same way. No difference in the mobility was seen between particles from asbestiform versus nonasbestiform minerals.

There is considerable scatter in the points in Fig. 1 because both the electrophoretic mobility and aspect ratio measurements were subject to rather large experimental uncertainties. The measured mobility has been found to be somewhat variable even for particles of the same dimensions, and the standard deviation for individual values of mobility was about ± 10 percent. Since the particles exhibited some Brownian movement during photographing, the images were seldom in sharp focus. Measurements of aspect ratios from the photographs had a standard deviation of ± 15 percent. Some additional error in determining particle length could have occurred when elongated particles were slightly nonparallel to the bottom of the cell.

The relation between electrophoretic mobility and aspect ratio in Fig. 1 appeared somewhat complex. In order to explain the observed behavior, an equation was derived based on the geometry of amphibole particles. This mathematical expression states that the net or overall charge per unit surface area is the sum of the charge per unit area of the different surface regions of each particle. A derivation of the equation is as follows.

The charged surface surrounding each amphibole particle at the Stern plane was assumed to be cylindrical in shape (5) with a radius r and length ℓ . The bases of the particles (cleavage planes perpendicular to the c -axis) were assumed to have a charge density, σ_1 , that could be different from the lateral charge density, σ_2 . The crystal structure of amphi-

Fig. 1. Electrophoretic mobility plotted as a function of the aspect ratio for grunerite asbestos, acicular tremolite, crocidolite, and riebeckite.



boles is such that surfaces would have different ionic composition at planes parallel to and perpendicular to the c -axis (6). Earlier work (1, 5) has indicated that neither fibers nor cleavage fragments have well-defined rectangular cross sections due to growth or cleavage along crystal planes. The average chemical composition of the lateral surfaces is assumed to be the same for both fibers and cleavage fragments; this assumption is substantiated by the fact that fibers and cleavage fragments have the same mobility when their dimensions are the same. Because of the different basal and lateral composition, the assumption of dissimilar charge densities appeared reasonable. Geometrical consideration of surface areas and surface charges in terms of aspect ratio leads to the following equations. The aspect ratio (γ) for a particle is defined as

$$\gamma = \frac{\ell}{2r} \quad (1)$$

The lateral surface area (A_ℓ) and the basal surface area (A_b), respectively, are given by

$$A_\ell = 2\pi r \ell = 4\pi r^2 \gamma, \quad A_b = 2\pi r^2 \quad (2)$$

The total surface charge (Q) is the sum of the products of the area multiplied by the corresponding charge densities σ_1 and σ_2 :

$$Q = \sigma_1 A_b + \sigma_2 A_\ell = \frac{2\pi r^2 \sigma_1 + 4\pi r^2 \gamma \sigma_2}{2\pi r^2 \sigma_1 + 4\pi r^2 \gamma \sigma_2} \quad (3)$$

The net surface charge density (σ) equals the total charge divided by the total area, thus

$$\sigma = \frac{Q}{A_\ell + A_b} = \frac{2\pi r^2 (\sigma_1 + 2\sigma_2 \gamma)}{4\pi r^2 \gamma + 2\pi r^2} = \frac{\sigma_1 + 2\sigma_2 \gamma}{2\gamma + 1} \quad (4)$$

Since electrophoretic mobility is essentially directly proportional to zeta po-

tential and in turn to the density of charge on the particle surface, multiplication of the charge densities in Eq. 4 by the appropriate constants gives an equation in terms of the electrophoretic mobilities (μ)

$$\mu = \frac{\mu_1 + 2\mu_2 \gamma}{2\gamma + 1} \quad (5)$$

The constants μ_1 and μ_2 are the limiting mobilities for the extreme cases of particle shape; μ_1 would be the mobility for a cylindrical wafer, and μ_2 would be the mobility for an infinitely long fiber. For every real particle, the observed mobility μ will be a combination of the mobilities resulting from the lateral and basal contributions. Although the above model is based on the cylindrical geometry of the particle, essentially the same relationship can be derived for particles in the form of rectangular parallelepipeds.

In order to evaluate the constants μ_1 and μ_2 , we carried out a linear regression analysis of the data for each material and for all the combined data, according to Eq. 5. Individual and average values of μ_1 and μ_2 are given in Table 1 for comparison, and we constructed the curve in Fig. 1 using the average values of μ_1 and μ_2 . There is remarkably good agreement between the trend of observed experimental values and the behavior predicted from Eq. 5. Because the curve has such a large slope at aspect ratios less than 1, values of μ_1 are somewhat unprecise. The exact magnitude of μ_1 is unimportant, but the difference in sign gives the curve its unique shape. A logarithmic or power-series equation might be fitted to the data points, but such an equation would be entirely empirical. The constants in Eq. 5 have physical significance as limiting values of μ .

Some earlier research has indicated that the surface composition and surface charge may be dissimilar for different

faces of crystals (7). The results presented here indicate that amphibole particles appear to have opposite surface charge on lateral and basal surfaces. Therefore, short amphibole fibers and blocky cleavage fragments have a smaller net charge than elongated fibers and cleavage fragments.

JOSEPH E. SCHILLER
SEQUOYAH L. PAYNE
SANAA E. KHALAFALLA

Twin Cities Research Center,
Bureau of Mines,
Post Office Box 1660,
Twin Cities, Minnesota 55111

References and Notes

1. J. E. Schiller and S. L. Payne, *U.S. Bur. Mines Rep. Invest.*, in press.
2. W. J. Campbell, R. L. Blake, L. L. Brown, E. E. Cather, J. J. Sjoberg, *U.S. Bur. Mines Inf. Circ. 8751* (1977).
3. V. Timbrell and R. E. G. Rendall, *Powder Technol.* **5**, 279 (1971-1972).
4. J. T. G. Overbeck and P. H. Wiersema, in *Electrophoresis*, M. Bier, Ed. (Academic Press, New York, 1967), pp. 1-52; D. Stigter, *J. Phys. Chem.* **82**, 1417 (1978).
5. M. A. Franco, J. L. Hutchison, D. A. Jefferson, J. M. Thomas, *Nature (London)* **266**, 520 (1977).
6. W. G. Ernst, *Minerals, Rocks, and Inorganic Materials*, vol. 1, *Amphiboles* (Springer-Verlag, New York, 1968), chap. 1.
7. J. H. Smolik and D. W. Fuerstenau, *Trans. Soc. Min. Eng. AIME* **235**, 367 (1966); H. Van Olphen, *An Introduction to Clay Colloid Chemistry* (Wiley, New York, ed. 2, 1977), pp. 94-95.

21 January 1980; revised 21 April 1980

Tetracycline-Labeled Human Bone from Ancient Sudanese Nubia (A.D. 350)

Abstract. Nubian bone recovered from an X-group cemetery (A.D. 350 to 550) exhibits a pattern of fluorescence identical to that of modern tetracycline-labeled bone. When it is viewed under ultraviolet light at 490 angstroms, fluorophors are visible as a characteristic yellow-green fluorescence on surfaces that were actively mineralizing at the time of exposure. Contamination of stored grains provided the proper environment for cultivation of tetracycline-producing *Streptomyces*. Evidence for exposure to antibiotics in an archeological population is relevant to studies of the evolution of R factors and to the interpretation of health and disease within the population.

When thin sections of compact bone from an archeological population of Sudanese Nubians were viewed under a fluorescence microscope, a pattern of fluorescence identical to that of modern tetracycline-labeled bone was observed (1). This bone predates the antibiotic era by at least 1400 years.

The prescribing of tetracyclines as broad-spectrum antibiotics in the 1950's led to the discovery that their use causes staining and fluorescence in calcifying tissues (2). In compact bone, tetracycline is bound to the surfaces of Haversian systems (osteons) actively mineralizing at the time of the administration of the drug; mature osteons remain unaffected. The tetracyclines are active ion chelators, forming complex calcium and protein compounds (3) that produce intense yellow-green fluorophors (2). This fluorescence persists through time (4) and has been useful in the analysis of bone dynamics (5).

The fluorophor-labeled bone was recovered from an X-group (6) cemetery on the west bank of the Nile River opposite the town of Wadi Halfa in the Sudan. The X-group (Ballana) period (A.D. 350 to 550) represents a phase of independent rule after the decline of the Meroitic Kingdom (350 B.C. to A.D. 350) and preceding the rise of Christianity (A.D. 550

to 1300) in Nubia. The X-group people were intensive agriculturalists, cultivating the floodplains of the Nile.

The X-group population has been extensively studied. Samples of both compact (7) and trabecular (8) bone were examined macroscopically. Microscopic examination of compact bone was carried out (9), and there was gross examination of dentition (10) and changes in cranial morphology (11). Patterns of pathology were related to the adaptation of the group (12).

The material was excavated in a state of excellent preservation—in most cases with hair and naturally mummified tissue adhering to the skeletons. Thin sections were taken from the area immediately distal to the lesser trochanter on 15 left femurs. The undecalcified, unembedded sections were mounted with Hillquist epoxy on petrographic slides (13), ground by hand to a thickness of 90 μm with carborundum paper of 320, 400, and 600 grit, and polished. The sections were viewed at 490 \AA with a fluorescence microscope (Reichert NR340101) with a darkfield VG-1 filter. Fluorescence was observed in all samples.

Serial extraction of collagen indicates little postmortem degradation. Analyses of hydroxyproline, proline, and mucopolysaccharides suggest that collagen

was present in levels comparable to that extracted from biopsy or autopsy material (14).

Several observations support the hypothesis that tetracycline caused the bone fluorescence. The fluorophors were visible at the same wavelength (490 \AA) and had the same color (yellow-green) as oxytetracycline-labeled bone. In addition, the pattern of fluorescence occurred in a manner histologically identical to that of labeling by tetracycline.

In vivo, tetracycline can only be deposited on actively mineralizing surfaces, forming a discernible pattern in osteons and across the cortical surface. Intense fluorescence corresponds to areas that were actively mineralizing at the time of exposure to the tetracyclines; low concentrations of fluorophors correspond to the areas that were mineralized later (15). The patterns of fluorescence in the X-group bone are directly comparable to those observed in modern tetracycline-labeled bone.

About 30 percent of all the osteons we observed contained fluorophors; some were completely fluorescent even though they were adjacent to nonfluorescing osteons (Fig. 1A). Most of the fluorescing osteons were located in the endosteal third of the compact bone. Femurs from older individuals showed some fluorescence in the subperiosteal area. No other age (or gender) pattern was discernible.

In most instances, fluorescence appeared as wide bands corresponding to the lamellar bone in the osteons (Fig. 1). In most of the labeled osteons, the brightest fluorescence was present in the inner one-third, followed by the outer and middle thirds. Areas of high mineral density surrounding Haversian canals fluoresced brightly (Fig. 1B); they correspond to the edge sclerosis seen in microradiographs.

Mineralization occurs on the subperiosteal and endosteal surfaces (16) as well as within osteons (17). Fluorescence was observed in the lacunae (Fig. 1), in the lamellae on the subperiosteal surface, and on the endosteal surface. In the diaphysis, fluorophors appeared as bands 5 to 10 μm in thickness on the subperiosteal and endosteal surfaces. In cross section, they formed concentric rings (18).

A small percentage of osteons exhibited "feathering," a phenomenon described by Frost (19) as incompletely mineralized bone matrix in humans. In vivo, this bone is relatively impermeable to tetracycline (19), the feathered portion not being labeled. Figure 1C depicts a